

Anomalous stopping of laser-accelerated intense proton beam in dense ionized matter

Jieru Ren,¹ Zhigang Deng,² Wei Qi,² Benzheng Chen,^{1,3} Bubo Ma,¹ Xing Wang,¹ Shuai Yin,¹ Jianhua Feng,¹ Wei Liu,^{1,4} Dieter H.H. Hoffmann,¹ Shaoyi Wang,² Quanping Fan,² Bo Cui,² Shukai He,² Zhurong Cao,² Zongqing Zhao,² Leifeng Cao,² Yuqiu Gu,² Shaoping Zhu,^{5,2,6} Rui Cheng,⁷ Xianming Zhou,^{1,8} Guoqing Xiao,⁷ Hongwei Zhao,⁷ Yihang Zhang,⁹ Zhe Zhang,⁹ Yutong Li,⁹ Dong Wu,^{3,*} Weimin Zhou,^{2,†} and Yongtao Zhao^{1,‡}

¹*MOE Key Laboratory for Nonequilibrium Synthesis and Modulation of Condensed Matter, School of Science, Xi'an Jiaotong University, Xi'an 710049, China*

²*Science and Technology on Plasma Physics Laboratory, Laser Fusion Research Center, China Academy of Engineering Physics, Mianyang 621900, China*

³*Institute for Fusion Theory and Simulation, Department of Physics, Zhejiang University, Hangzhou 310058, China*

⁴*Xi'an Technological University, Xi'an 710021, China*

⁵*Institute of Applied Physics and Computational Mathematics, Beijing 100094, China*

⁶*Graduate School, China Academy of Engineering Physics, Beijing 100088, China*

⁷*Institute of Modern Physics, Chinese Academy of Sciences, Lanzhou 710049, China*

⁸*Xianyang Normal University, Xianyang 712000, China*

⁹*Institute of Physics, Chinese Academy of Sciences, Beijing 100190, China*

(Dated: January 31, 2022)

Ultrahigh-intensity lasers (10^{18} - 10^{22} W/cm²) have opened up new perspectives in many fields of research and application [1–5]. By irradiating a thin foil, an ultrahigh accelerating field (10^{12} V/m) can be formed and multi-MeV ions with unprecedentedly high intensity (10^{10} A/cm²) in short time scale (\sim ps) are produced [6–14]. Such beams provide new options in radiography [15], high-yield neutron sources [16], high-energy-density-matter generation [17], and ion fast ignition [18, 19]. An accurate understanding of the nonlinear behavior of beam transport in matter is crucial for all these applications. We report here the first experimental evidence of anomalous stopping of a laser-generated high-current proton beam in well-characterized dense ionized matter. The observed stopping power is one order of magnitude higher than single-particle slowing-down theory predictions. We attribute this phenomenon to collective effects where the intense beam drives an decelerating electric field approaching 1GV/m in the dense ionized matter. This finding will have considerable impact on the future path to inertial fusion energy.

Alpha particle stopping in dense ionized matter is essential to achieve ignition in inertial confinement fusion [20–24]. Fast ignition (FI) relies even more on a detailed understanding of ultrahigh-current ion stopping in matter, which is therefore considered as a fundamental process of utmost importance to nuclear fusion. In the fast ignition scheme [25, 26], a short and intense pulse of energetic charged particles - electrons, protons or heavy ions - generated by an ultrahigh intensity laser, is directed towards the pre-compressed fusion pellet. The charged-particle beam requirements to achieve ignition have been discussed and studied in detail previously [27–31] based on single-particle stopping theory. However, the collective effects induced by high-current charged particle beams could alter significantly the projected range, the magnitude of energy deposition, and therefore change the requirements for ignition correspondingly. Besides, in the cases of ion beam driven inertial confinement fusion and high energy density science, which requires the highest beam intensity from accelerators [32–36], no collective effects on ion stopping processes due to high beam intensity are considered nor - to the best of our knowledge - were they reported in any previous experiments.

Since the discovery of alpha decay and the availability of energetic fission fragments, it became interesting to study fast particle stopping processes in matter [37]. In

past decades, numerous theoretical models [38–44], some of which can be considered to be further developments of the early work of Bethe [40] and Bloch [41], are built to describe single charged particle stopping in dense ionized matter. Only recently experiments with sufficient precision were carried out with dense ionized matter to distinguish between different models [45–47]. In these experiments, incident particles are generated from laser induced nuclear reactions [45, 46], or from traditional accelerators [47]. Hence the beam intensity was too low to test the model of single particles interacting with dense ionized matter.

Intense particle beams generated from interaction of ultrahigh intensity laser with foil open a new realm, where beam-driven complex collective phenomena are expected to occur [48–53]. In particular, the stopping power for these intense beam could be orders of magnitude higher than that for individual particles if the beam intensity is high enough [54–57]. We ever carried out an experiment in previous, and observed a significant enhancement of energy loss for the laser-accelerated intense proton beam (see [58] and supplementary material for details). However, it was difficult to conduct quantitative analysis due to the large energy spread of the beam. In order to improve our understanding of these effects, experimental data with high precision are required.

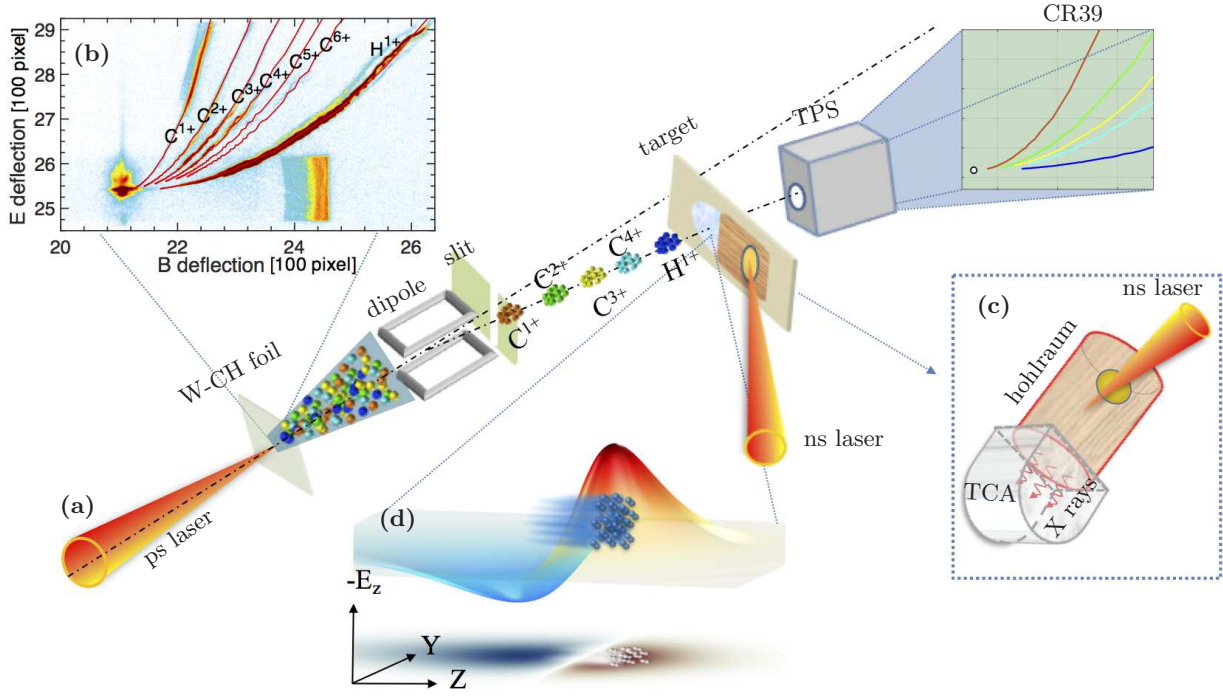


FIG. 1. **Layout of the experiment.** (a) A ps laser is focused onto a tungsten foil, generating intense short-pulse ion beams with different species. A magnetic dipole with slits at entrance and exit serve as p/q analyser to select mono-energetic ion beams. Such ions interact with the laser generated plasma-target and emerge from the target with a lower energy due to the incurred energy loss. The final-state energy is measured by a Thomson parabola in conjunction with CR39 film. (b) Parabola spectra of laser-accelerated ions without dipole measured by Thomson parabola in conjunction with Fuji image plate. (c) The target consists of a gold hohlraum converter to produce the soft x-rays that irradiate the TCA foam to generate a dense ionized sample. (d) The insert shows the simulation result of an intense proton beam moving along the z direction, inducing a strong longitudinal electric field, which is counter-directional to the proton beam propagation, causing anomalous stopping.

Here in this work, we improve the precision of the measurements through using a magnetic dipole to trim out a quasi-mono-energetic proton beam with energy spread of $\sim 6\%$. The dense ionized matter was produced from irradiating a Tri-Cellulose Acetate (TCA) foam sample with soft x-rays from a laser-heated hohlraum. The hydrodynamic timescale of the target is long compared to the proton beam pulse, hence the target can be considered to be quasi static with well-characterized parameters. This is able to quantitatively study the anomalous stopping of intense beam in dense ionized matter. We observed enhanced stopping by one order of magnitude compared to the classical single particle slowing-down theory. We attribute this phenomenon to a strong decelerating electric field induced by the intense proton beam. Our numerical simulation indicates that this collective effect is the primary cause for the anomalous stopping, and it is likely to have a major impact on nuclear fusion scenarios like fast ignition, alpha-particle self heating, as well as ion driven inertial confinement fusion.

EXPERIMENTAL SETUP AND DATA TAKING

The experiment was carried out at the XG-III laser facility of Laser Fusion Research Center in Mianyang. The experimental layout is displayed in Fig. 1. Here a short and intense laser beam of 800 fs duration, 20 μm focal spot and 150 J total energy irradiates a CH-coated tungsten foil (15 μm -thick), generating charged particle beam. The beam consists of a mixture of protons (H^{1+}) and carbon ions with different charge states (C^{1+} , C^{2+} , C^{3+} and C^{4+}). They originate at the backside of the target by means of the target normal sheath acceleration (TNSA). The predominant particle species is H^{1+} , because the charge to mass ratio is maximum for this species and is therefore more effectively accelerated than the lower charge-to-mass ratio species of carbon ions. In view that the TNSA mechanism results in a broad range of particle energies, which is not favorable for quantitative analysis of the particle energy loss. A magnetic dipole, with entrance and exit slits, was used to trim the beam to mono-energetic one. The ions, spatially collimated by the 500 μm entrance slit, are dispersed laterally by the magnetic dipole according to their specific

\mathbf{p}/q value, where p and q are the particle momentum and charge respectively. A second $500\ \mu\text{m}$ exit slit, selects the quasi-mono-energetic ion pulses. The selected ions consist of different particle species, with similar \mathbf{p}/q value, they have, however, different velocities and therefore arrive at the target pulse by pulse with different time delay.

A gold hohlraum converter was used to generate soft x-ray radiation by interaction of a ns laser pulse [150 J], with the hohlraum walls. The X rays subsequently irradiated and heated the foam target ($\text{C}_9\text{H}_{16}\text{O}_8$, density of $2\ \text{mg}/\text{cm}^{-3}$ and thickness of $1\ \text{mm}$), into ionized state. Due to the large penetration of soft x-rays, the foam was heated quasi isochorically. The hydrodynamic response of this target material is very well investigated previously [59–61]. The hydrodynamic response time is in the ns regime, which is long compared to the proton pulse, hence the target can be considered to be quasi static with well-characterized plasma properties. In order to determine plasma parameters, the emission spectra of the gold hohlraum and target matter were measured. The gold hohlraum radiation spectrum is well represented by a 20 eV black body radiation spectrum, while the temperature of the plasma target is 17 eV. This value was obtained from a Boltzmann slope analysis of the He like carbon lines. Given a temperature of 17 eV, and mass density of $2\ \text{mg}/\text{cm}^{-3}$, the number density of free electrons is determined to be $4 \times 10^{20}\ \text{cm}^{-3}$ based on the FLYCHK code [62].

A thomson parabola spectrometer (TPS) in conjunction with a plastic track detector CR39 was used to obtain the energy spectrum of the charged particles. In Fig. 2(a), tracks recorded on CR39 film are displayed for ions passing through the system with/without target.

When the plasma target is inserted, only protons are observed in the TPS. The deflection distances of protons without/with target are converted to energies in Fig. 2(b) and (c), respectively. The incident, unperturbed protons without target appear at 3.36 MeV with a half width of the distribution (FWHM) of 0.06 MeV. Protons passing through the plasma target are downshifted in energy to 2.98 MeV and the FWHM increased to 0.20 MeV.

DISCUSSION

In Fig. 3, the measured energy loss is compared to theoretical models, e.g. Bethe-Bloch model, Li-Petrasso (LP) theory [38] and Standard Stopping Model (SSM) by Deutsch [44]. These theories are based on binary collisions with free electrons, bound electrons and/or plasmons. They all underestimate the measured stopping power by as much as one order of magnitude. We therefore call the observed effect anomalous stopping and attribute this to collective electromagnetic effects induced by high-current ion beams.

In order to understand this anomalous stopping, both collective electromagnetic effects and close particle-particle interactions need to be taken into account. The most appropriate tool to simulate the conditions of the experiment is the Particle-in-Cell method (PIC), which in recent years has established itself as a state-of-the-art method for solving problems of kinetic plasma physics.

The simulation assumes, the incident proton beam to have Gaussian distribution in space and time, with a beam duration of 1 ps and a transverse extension of 1 mm. The energy spectrum is also assumed to be Gaussian, with the peak of the energy distribution at 3.36 MeV and FWHM of 0.06 MeV. The measured ionized target parameters were used as simulation input. The simulation was carried out in Z-Y Cartesian geometry with beam propagating along the Z-direction. The size of the simulation box was $1.2\ \text{mm} \times 2.5\ \text{mm}$, with a grid size of $0.75\ \mu\text{m} \times 25\ \mu\text{m}$, containing 25 particles per grid for each plasma species and 64 particles per grid for the proton beam.

Given the incident proton beam with density of $8 \times 10^{16}\ \text{cm}^{-3}$, which corresponds to high-current case of $3.2 \times 10^7\ \text{A}/\text{cm}^2$, Fig. 4(a) shows the longitudinal electric field E_z induced by the beam-driven return current after a propagation distance of about 0.3 mm. A strong decelerating field approaching $10^9\ \text{V}/\text{m}$ is generated, and contributes to the proton stopping. The proton energy spectrum after passing through 1 mm of plasma is shown in Fig. 4(c). The energy spread is significantly broadened compared to the initial spread. We attribute this to a decreasing field, the protons are imbedded in. Protons with higher energies are located at the front end of bunch and therefore experience a smaller decelerating electric field than those with lower energies that come later. The spatial size of this decelerating field is comparable to size of the proton bunch. This is different from the plasma wakefield case [63, 64], where the spatial structure of the electric field is determined by the plasma density. Here the plasma wakefield wavelength is much smaller than the beam length, therefore the wakefield-induced collective acceleration and deceleration cancel out. The peak energy of protons is downshifted by 0.39 MeV after passing through the plasma. As shown in Fig. 3, this energy shift (blue triangle) agrees with experimental data in magnitude. We carried out additional simulations for different beam densities at $8 \times 10^{11}\ \text{cm}^{-3}$ and $8 \times 10^{15}\ \text{cm}^{-3}$, which are defined as low- and intermediate-current cases, respectively. For the low-current case, the beam induced longitudinal electric field E_z after propagating for 0.3 mm in the plasma is shown in Fig. 4(b). No collective decelerating field is excited under such conditions. After passing through the plasma, the energy spectrum is downshifted by only 0.02 MeV as shown in Fig. 4(c). This prediction agrees well with those calculated by the different binary collision theories, as shown in Fig. 3., which indicates the dominant role of collisional stopping

in low-current cases. As for the intermediate case, the stopping due to the collective effects are comparable to that caused by binary collisions, giving rise to an energy loss of 0.04 MeV as shown in Fig. 4(c).

Therefore, the energy loss of laser-accelerated proton beam in the current dense ionized matter is composed of two terms as $dE/dx = (dE/dx)_{\text{collision}} + (dE/dx)_{\text{collective}}$. The first term $(dE/dx)_{\text{collision}}$ describes the collisional stopping induced by atomic binary interaction of the individual projectiles with the individual particles in the plasma, which is well predicted by the classic Bethe-Bloch equation and other traditional binary collision theories. The second term $(dE/dx)_{\text{collective}}$ describes the collective stopping induced by the self-formed deceleration field, that occurs when sending a very dense ion bunch into the plasma. Since the ion bunch is imbedded in the deceleration field that increases with the increasing ion bunch density, we expect a significant enhancement of the energy loss (here measured as 20 fold) in the plasma for a very dense ion bunch compared with individual particles incidence.

CONCLUSION

In summary, the laser-accelerated intense proton beam stopping in a dense ionized matter has been measured. Benefiting from the fact that we have a quasi-monoenergetic proton beam and long-living well-characterized dense ionized target, accurate stopping power data were obtained. The measured stopping power exceeds the classical theory predicts in binary collision scheme by about one order of magnitude. The anomalous phenomena can be very well explained by our PIC simulation combined with a new Monte Carlo binary collision model and a reduced model taking account the collective electromagnetic effects. The stopping power is dramatically enhanced due to the return-current-induced decelerating electric field approaching 1GV/m. We have demonstrated the existence of collective effects, for high density beam, leading to enhanced stopping. This phenomenon will be important for the optimum design of ion driven inertial confinement fusion and fast ignition scenarios.

METHOD

We used the newly developed PIC code LAPINS [65, 66], where close interactions including proton-nuclei, proton-bound electron, proton-free electron were treated by a Monte Carlo binary collision model [67]. Furthermore a new Monte Carlo ionization dynamics model was added [68], including collisional ionization, electron-ion recombination and ionization potential depression. Simulation of large scale plasmas often results in an intractable

burden on computer power. Therefore, instead of solving the full Maxwell's equations, we used a new approach by combining the PIC method with a reduced model [65]. To take into account collective electromagnetic effects, the background electron inertia is neglected, and instead the background return current is evaluated by the Ampere's law $\mathbf{J}_e = (1/2\pi)\nabla \times \mathbf{B} - (1/2\pi)\partial\mathbf{E}/\partial t - \mathbf{J}_b - \mathbf{J}_i$, where \mathbf{B} is the magnetic field, \mathbf{E} is the electric field, and \mathbf{J}_i is the background ion current. Applying the continuity equation $\nabla \cdot \mathbf{J} + \partial\rho/\partial t = 0$ with the total current $\mathbf{J} = \mathbf{J}_b + \mathbf{J}_i + \mathbf{J}_e$, the Poisson Equation $\nabla \cdot \mathbf{E} = 2\pi\rho$ is rigorously satisfied. The electric fields are then obtained from Ohm's law, $\mathbf{E} = \eta\mathbf{J}_e - \mathbf{v}_e \times \mathbf{B}$, where \mathbf{v}_e is the background electron velocity, and η is the resistivity. Taking advantage of the Monte Carlo collision model, resistivity η is obtained by averaging over all binary collisions at each time step for each simulation cell. Finally, Faraday's law is used to obtain the magnetic fields $\partial\mathbf{B}/\partial t = -\nabla \times \mathbf{E}$. This field solver, which couples Ampere's law, Faraday's law and Ohm's law, can completely remove the numerical heating and reduces significantly the numerical expense. With these advantageous features a unique tool is at hand, which can self-consistently model transport and energy deposition of intense charged particles in dense ionized matter.

* dwu.phys@zju.edu.cn

† zhouwm@caep.cn

‡ zhaoyongtao@xjtu.edu.cn

- [1] J R Rygg, F H Seguin, C K Li, J A Frenje, M J E Manuel, R D Petrasso, R Betti, J A Delettrez, O V Gotchev, J P Knauer, et al. Proton radiography of inertial fusion implosions. *Science*, 319(5867):1223–1225, 2008.
- [2] Y J Gu, Ondrej Klimo, S V Bulanov, and Stefan Weber. Brilliant gamma-ray beam and electron-positron pair production by enhanced attosecond pulses. *Communications in Physics*, 1(1):1–9, 2018.
- [3] Marija Vranic, Ondrej Klimo, Georg Korn, and Stefan Weber. Multi-gev electron-positron beam generation from laser-electron scattering. *Scientific Reports*, 8(1):4702–4702, 2018.
- [4] Li Yan-Fei, Shaisultanov Rashid, Chen Yue-Yue, Wan Feng, Hatsagortsyan Karen Z., Keitel Christoph H., and Li Jian-Xing. Polarized ultrashort brilliant multi-gev gamma-rays via single-shot laser-electron interaction. *Physical Review Letters*, 124:014801, 2020.
- [5] R Kodama, P A Norreys, Kunioki Mima, A E Dangor, R G Evans, H Fujita, Yoneyoshi Kitagawa, K Krushelnick, T Miyakoshi, N Miyanaga, et al. Fast heating of ultrahigh-density plasma as a step towards laser fusion ignition. *Nature*, 412(6849):798–802, 2001.
- [6] Teresa Bartal, Mark E Foord, Claudio Bellei, Michael H Key, Kirk A Flippo, Sandrine A Gaillard, Dustin T Offermann, Pravesh K Patel, Leonard C Jarrott, Drew P Higginson, et al. Focusing of short-pulse high-intensity laser-accelerated proton beams. *Nature Physics*, 8(2):139, 2012.

- [7] Björn Manuel Hegelich, BJ Albright, J Cobble, K Flippo, S Letzring, M Paffett, H Ruhl, Jörg Schreiber, RK Schulze, and JC Fernández. Laser acceleration of quasi-monoenergetic mev ion beams. *Nature*, 439(7075):441, 2006.
- [8] T E Cowan, J Fuchs, H Ruhl, A J Kemp, P Audebert, M Roth, R B Stephens, I Barton, A Blazevic, E Brambrink, et al. Ultralow emittance, multi-mev proton beams from a laser virtual-cathode plasma accelerator. *Physical Review Letters*, 92(20):204801–204801, 2004.
- [9] M Roth, A Blazevic, Matthias Geissel, Theodor Schlegel, T E Cowan, M Allen, Jeanclaude Gauthier, Patrick Audebert, J Fuchs, J Meyertervehn, et al. Energetic ions generated by laser pulses: A detailed study on target properties. *Physical Review Special Topics-accelerators and Beams*, 5(6):061301, 2002.
- [10] M Hegelich, Stefan Karsch, Georg Pretzler, D Habs, Klaus Witte, W Guenther, M Allen, A Blazevic, J Fuchs, Jeanclaude Gauthier, et al. Mev ion jets from short-pulse-laser interaction with thin foils. *Physical Review Letters*, 89(8):085002–085002, 2002.
- [11] Stephen P Hatchett, C G Brown, T E Cowan, Eugene A Henry, Joy S Johnson, Michael H Key, J A Koch, A Bruce Langdon, B F Lasinski, R W Lee, et al. Electron, photon, and ion beams from the relativistic interaction of petawatt laser pulses with solid targets. *Physics of Plasmas*, 7(5):2076–2082, 2000.
- [12] R Snavely, M H Key, S P Hatchett, T E Cowan, M Roth, T W Phillips, M A Stoyer, E A Henry, T C Sangster, M S Singh, et al. Intense high-energy proton beams from petawatt-laser irradiation of solids. *Physical Review Letters*, 85(14):2945–2948, 2000.
- [13] A Maksimchuk, S Gu, K A Flippo, Donald P Umstadter, and V Yu Bychenkov. Forward ion acceleration in thin films driven by a high-intensity laser. *Physical Review Letters*, 84(18):4108–4111, 2000.
- [14] Zhengming Sheng, Y Sentoku, K Mima, J Zhang, Wei Yu, and J Meyertervehn. Angular distributions of fast electrons, ions, and bremsstrahlung x/gamma-rays in intense laser interaction with solid targets. *Physical Review Letters*, 85(25):5340–5343, 2000.
- [15] J A Cobble, R P Johnson, T E Cowan, N Renardle Galoudec, and M Allen. High resolution laser-driven proton radiography. *Journal of Applied Physics*, 92(4):1775–1779, 2002.
- [16] M. Roth, D. Jung, K. Falk, N. Guler, O. Deppert, M. Devlin, A. Favalli, J. Fernandez, D. Gautier, M. Geissel, R. Haight, C. E. Hamilton, B. M. Hegelich, R. P. Johnson, F. Merrill, G. Schaumann, K. Schoenberg, M. Schollmeier, T. Shimada, T. Taddeucci, J. L. Tybo, F. Wagner, S. A. Wender, C. H. Wilde, and G. A. Wurden. Bright laser-driven neutron source based on the relativistic transparency of solids. *Phys. Rev. Lett.*, 110:044802, Jan 2013.
- [17] P K Patel, Andrew Mackinnon, M H Key, T E Cowan, M E Foord, M Allen, D Price, H Ruhl, P T Springer, and R B Stephens. Isochoric heating of solid-density matter with an ultrafast proton beam. *Physical Review Letters*, 91(12):125004, 2003.
- [18] M Roth, T E Cowan, M H Key, S P Hatchett, C Brown, W F Fountain, J Johnson, D M Pennington, R A Snavely, S C Wilks, et al. Fast ignition by intense laser-accelerated proton beams. *Physical Review Letters*, 86(3):436–439, 2001.
- [19] Weimin Wang, Paul Gibbon, Zhengming Sheng, and Yutong Li. Magnetically assisted fast ignition. *Physical Review Letters*, 114(1):015001, 2015.
- [20] OA Hurricane, DA Callahan, DT Casey, EL Dewald, TR Dittrich, T Döppner, S Haan, DE Hinkel, LF Berzak Hopkins, O Jones, et al. Inertially confined fusion plasmas dominated by alpha-particle self-heating. *Nature Physics*, 12(8):800, 2016.
- [21] Stefano Atzeni and Jürgen Meyer-ter Vehn. *The physics of inertial fusion: beam plasma interaction, hydrodynamics, hot dense matter*, volume 125. OUP Oxford, 2004.
- [22] J Paradela, F García-Rubio, and J Sanz. Alpha heating enhancement in maglif targets: A simple analytic model. *Physics of Plasmas*, 26(1):012705, 2019.
- [23] R Betti and OA Hurricane. Inertial-confinement fusion with lasers. *Nature Physics*, 12(5):435, 2016.
- [24] S Jacquemot. Inertial confinement fusion for energy: overview of the ongoing experimental, theoretical and numerical studies. *Nuclear Fusion*, 57(10):102024, 2017.
- [25] NG Basov, S Yu Gus'kov, and LP Feokistov. Thermonuclear gain of icf targets with direct heating of ignitor. *Journal of Soviet Laser Research*, 13(5):396–399, 1992.
- [26] Max Tabak, James Hammer, Michael E Glinsky, William L Kruer, Scott C Wilks, John Woodworth, E Michael Campbell, Michael D Perry, and Rodney J Mason. Ignition and high gain with ultrapowerful lasers. *Physics of Plasmas*, 1(5):1626–1634, 1994.
- [27] Juan C Fernández, JJ Honrubia, Brian J Albright, Kirk A Flippo, D Cort Gautier, Björn M Hegelich, Mark J Schmitt, M Temporal, and Lin Yin. Progress and prospects of ion-driven fast ignition. *Nuclear fusion*, 49(6):065004, 2009.
- [28] H Nagatomo, T Johzaki, T Asahina, M Hata, Y Sentoku, K Mima, and H Sakagami. Study of fast ignition target design for ignition and burning experiments. *Nuclear Fusion*, 59(10):106055, 2019.
- [29] N Ratan, NJ Sircombe, L Ceurvorst, J Sadler, MF Kasim, J Holloway, MC Levy, R Trines, R Bingham, and PA Norreys. Dense plasma heating by crossing relativistic electron beams. *Physical Review E*, 95(1):013211, 2017.
- [30] T Yanagawa, H Sakagami, A Sunahara, and H Nagatomo. Asymmetric implosion of a cone-guided target irradiated by gekko xii laser. *Laser and Particle Beams*, 33(3):367–378, 2015.
- [31] M Temporal, R Ramis, B Canaud, V Brandon, S Lafite, and BJ Le Garrec. Irradiation uniformity of directly driven inertial confinement fusion targets in the context of the shock-ignition scheme. *Plasma Physics and Controlled Fusion*, 53(12):124008, 2011.
- [32] Ingo Hofmann. Review of accelerator driven heavy ion nuclear fusion. *Matter and Radiation at Extremes*, 3(1):1–11, 2018.
- [33] A. Pelka, G. Gregori, D. O. Gericke, J. Vorberger, S. H. Glenzer, M. M. Günther, K. Harres, R. Heathcote, A. L. Kritcher, N. L. Kugland, B. Li, M. Makita, J. Mithen, D. Neely, C. Niemann, A. Otten, D. Riley, G. Schaumann, M. Schollmeier, An. Tauschwitz, and M. Roth. Ultrafast melting of carbon induced by intense proton beams. *Phys. Rev. Lett.*, 105:265701, Dec 2010.
- [34] DHH Hoffmann, VE Fortov, IV Lomonosov, V Mintsev, NA Tahir, D Varentsov, and J Wieser. Unique capabilities of an intense heavy ion beam as a tool for equation-of-state studies. *Physics of Plasmas*, 9(9):3651–3654, 2002.

- [35] V Mintsev, V Kim, I Lomonosov, D Nikolaev, A Ostrik, N Shilkina, A Shutov, V Ternovoi, D Yuriev, V Fortov, et al. Non-ideal plasma and early experiments at fair: HiHex-heavy ion heating and expansion. *Contributions to Plasma Physics*, 56(3-4):281–285, 2016.
- [36] J Ren, C Maurer, P Katrik, PM Lang, AA Golubev, V Mintsev, Y Zhao, and DHH Hoffmann. Accelerator-driven high-energy-density physics: Status and chances. *Contributions to Plasma Physics*, 58(2-3):82–92, 2018.
- [37] J F Ziegler. Stopping of energetic light ions in elemental matter. *Journal of Applied Physics*, 85(3):1249–1272, 1999.
- [38] Chi-Kang Li and Richard D Petrasso. Fokker-planck equation for moderately coupled plasmas. *Physical review letters*, 70(20):3063, 1993.
- [39] Gilles Maynard and Claude Deutsch. Born random phase approximation for ion stopping in an arbitrarily degenerate electron fluid. *Journal de Physique*, 46(7):1113–1122, 1985.
- [40] Hans Bethe. Zur theorie des durchgangs schneller korpuskularstrahlen durch materie. *Annalen der Physik*, 397(3):325–400, 1930.
- [41] Felix Bloch. Zur bremsung rasch bewegter teilchen beim durchgang durch materie. *Annalen der Physik*, 408(3):285–320, 1933.
- [42] Lowell S Brown, Dean L Preston, and Robert L Singleton Jr. Charged particle motion in a highly ionized plasma. *Physics Reports*, 410(4):237–333, 2005.
- [43] Dirk O Gericke. Stopping power for strong beam-plasma coupling. *Laser and Particle Beams*, 20(3):471–474, 2002.
- [44] Claude Deutsch and Gilles Maynard. Ion stopping in dense plasmas: a basic physics approach. *Matter and Radiation at Extremes*, 1(6):277, 2018.
- [45] JA Frenje, R Florido, R Mancini, T Nagayama, PE Grabowski, H Rinderknecht, H Sio, A Zylstra, M Gatu Johnson, CK Li, et al. Experimental validation of low-z ion-stopping formalisms around the bragg peak in high-energy-density plasmas. *Physical review letters*, 122(1):015002, 2019.
- [46] AB Zylstra, JA Frenje, PE Grabowski, CK Li, GW Collins, P Fitzsimmons, S Glenzer, F Graziani, SB Hansen, SX Hu, et al. Measurement of charged-particle stopping in warm dense plasma. *Physical review letters*, 114(21):215002, 2015.
- [47] W Cayzac, A Frank, A Ortner, V Bagnoud, MM Basko, S Bedacht, C Bläser, A Blažević, S Busold, O Deppert, et al. Experimental discrimination of ion stopping models near the bragg peak in highly ionized matter. *Nature communications*, 8:15693, 2017.
- [48] J Kim, B Qiao, C McGuffey, MS Wei, PE Grabowski, and FN Beg. Self-consistent simulation of transport and energy deposition of intense laser-accelerated proton beams in solid-density matter. *Physical review letters*, 115(5):054801, 2015.
- [49] SN Chen, S Atzeni, T Gangolf, M Gauthier, DP Higginson, R Hua, J Kim, F Mangia, C McGuffey, J-R Marquès, et al. Experimental evidence for the enhanced and reduced stopping regimes for protons propagating through hot plasmas. *Scientific reports*, 8(1):14586, 2018.
- [50] Shao-wei Chou, Jia Xu, K Khrennikov, Daniel E Cardenas, J Wenz, M Heigoldt, Luisa Hofmann, László Veisz, Stefan Karsch, et al. Collective deceleration of laser-driven electron bunches. *Physical review letters*, 117(14):144801, 2016.
- [51] M Honda, J Meyer-ter Vehn, and A Pukhov. Collective stopping and ion heating in relativistic-electron-beam transport for fast ignition. *Physical review letters*, 85(10):2128, 2000.
- [52] M Tatarakis, FN Beg, EL Clark, AE Dangor, RD Edwards, RG Evans, TJ Goldsack, KWD Ledingham, PA Norreys, MA Sinclair, et al. Propagation instabilities of high-intensity laser-produced electron beams. *Physical review letters*, 90(17):175001, 2003.
- [53] B Vauzour, A Debayle, X Vaisseau, S Hulin, H-P Schlenvoigt, D Batani, SD Baton, JJ Honrubia, Ph Nicolai, FN Beg, et al. Unraveling resistive versus collisional contributions to relativistic electron beam stopping power in cold-solid and in warm-dense plasmas. *Physics of Plasmas*, 21(3):033101, 2014.
- [54] R A Mccorkle and G J Iafrate. Beam-density effect on the stopping of fast charged particles in matter. *Physical Review Letters*, 39(26):1691–1691, 1977.
- [55] S Kawata, C Deutsch, and Y J Gu. Peculiar behavior of si cluster ions in a high-energy-density solid al plasma. *Physical Review E*, 99(1), 2019.
- [56] C Deutsch. Interaction of ion cluster beams with cold matter and dense plasmas. *Laser and Particle Beams*, 8(4):541–553, 1990.
- [57] D W Rule and Oakley H Crawford. Nature of the beam-density effect on energy loss by nonrelativistic charged-particle beams. *Physical Review Letters*, 52(11):934–937, 1984.
- [58] Y Zhao, W Liu, X Wang, R Cheng, X Zhou, Z Deng, S Wang, Q Fan, W Qi, Y Zhang, Z Zhang, W Zhou, L Cao, Y Gu, and Y Li. Stopping of laser-accelerated ion beam in a foam-plasma. *GSI-2018-2 REPORT: News and Reports from High Energy Density generated by Heavy Ion and Laser Beams*, page 35, 2018.
- [59] ON Rosmej, V Bagnoud, U Eisenbarth, V Vatulina, N Zhidkov, N Suslov, A Kunin, A Pinegin, D Schäfer, Th Nisius, et al. Heating of low-density cho-foam layers by means of soft x-rays. *Nuclear Instruments and Methods in Physics Research Section A: Accelerators, Spectrometers, Detectors and Associated Equipment*, 653(1):52–57, 2011.
- [60] ON Rosmej, N Suslov, D Martsovenko, G Vergunova, N Borisenko, N Orlov, T Rienecker, D Klir, K Rezack, A Orekhov, et al. The hydrodynamic and radiative properties of low-density foams heated by x-rays. *Plasma Physics and Controlled Fusion*, 57(9):094001, 2015.
- [61] Steffen Faik, Anna Tauschwitz, Mikhail M Basko, Joachim A Maruhn, Olga Rosmej, Tim Rienecker, Vladimir G Novikov, and Alexander S Grushin. Creation of a homogeneous plasma column by means of hohlraum radiation for ion-stopping measurements. *High energy density physics*, 10:47–55, 2014.
- [62] H-K Chung, MH Chen, WL Morgan, Yu Ralchenko, and RW Lee. Flychk: Generalized population kinetics and spectral model for rapid spectroscopic analysis for all elements. *High energy density physics*, 1(1):3–12, 2005.
- [63] C Huang, W Lu, M Zhou, CE Clayton, C Joshi, WB Mori, P Muggli, S Deng, E Oz, T Katsouleas, et al. Hosing instability in the blow-out regime for plasma-wakefield acceleration. *Physical review letters*, 99(25):255001, 2007.
- [64] E Adli, Arun Ahuja, O Apsimon, Robert Apsimon, A M Bachmann, D Barrientos, F Batsch, J Bauche, V K Berglyd Olsen, M Bernardini, et al. Acceleration

of electrons in the plasma wakefield of a proton bunch. *Nature*, 561(7723):363–367, 2018.

- [65] D Wu, W Yu, S Fritzsche, and XT He. High-order implicit particle-in-cell method for plasma simulations at solid densities. *Physical Review E*, 100(1):013207, 2019.
- [66] D Wu, XT He, W Yu, and S Fritzsche. Particle-in-cell simulations of laser–plasma interactions at solid densities and relativistic intensities: the role of atomic processes. *High Power Laser Science and Engineering*, 6, 2018.
- [67] D Wu, XT He, W Yu, and S Fritzsche. Monte carlo approach to calculate proton stopping in warm dense matter within particle-in-cell simulations. *Physical Review E*, 95(2):023207, 2017.
- [68] D Wu, XT He, W Yu, and S Fritzsche. Monte carlo approach to calculate ionization dynamics of hot solid-density plasmas within particle-in-cell simulations. *Physical Review E*, 95(2):023208, 2017.

ACKNOWLEDGEMENT

We sincerely thank Olga Rosmej from GSI Helmholtzzentrum für Schwerionenforschung for the physical discussion, as well as the staff from Laser Fusion Research Center, Mianyang for the laser system running and target fabrication. The work is supported by Chinese Science Challenge Project No. TZ2016005, National Key Research and Development Project No. 2019YFA0404900, National Natural Science Foundation of China (Grant Numbers 11705141, 11775282, and U1532263), and China Postdoctoral Science Foundation (Grant Numbers 2017M623145 and 2018M643613).

AUTHOR CONTRIBUTIONS

Yongtao Zhao conceived this work, organized the experiments and simulations with Weimin Zhou and Dong Wu, respectively. Jieru Ren, Zhigang Deng and Yongtao Zhao carried out the experiment together with the high power laser team (Zongqing Zhao, Weimin Zhou, and Yuqiu Gu), the plasma diagnostics team (Shaoyi Wang, Quanping Fan, Bubo Ma, Bo Cui, Xing Wang, Zhurong Cao and Leifeng Cao), ion beam characterization team (Wei Qi, Shuai Yin, Shukai He, Wei Liu, Rui Cheng, Xianming Zhou, Jianhua Feng, Yihang Zhang, and Zhe Zhang). Jieru Ren, Zhigang Deng, Shuai Yin, Wei Qi, Shaoyi Wang, and Quanping Fan analyzed the main part of the experimental data. Benzhen Chen, Jieru Ren, Yongtao Zhao and Dong Wu performed the simulations and related analysis. Shaoping Zhu, Guoqing Xiao, Hongwei Zhao, Yutong Li, Yuqiu Gu and Leifeng Cao contribute in the physical discussion. Jieru Ren, Yongtao Zhao, Dong Wu and Dieter Hoffmann wrote the paper.

DATA AVAILABILITY

The dataset generated and analyzed during the current study are available from the corresponding authors upon reasonable request. The simulation details are available from the corresponding author on reasonable request.

ADDITIONAL INFORMATION

Supplementary information is available in the online version of the paper.

COMPETING INTEREST

The authors declare no competing financial interests.

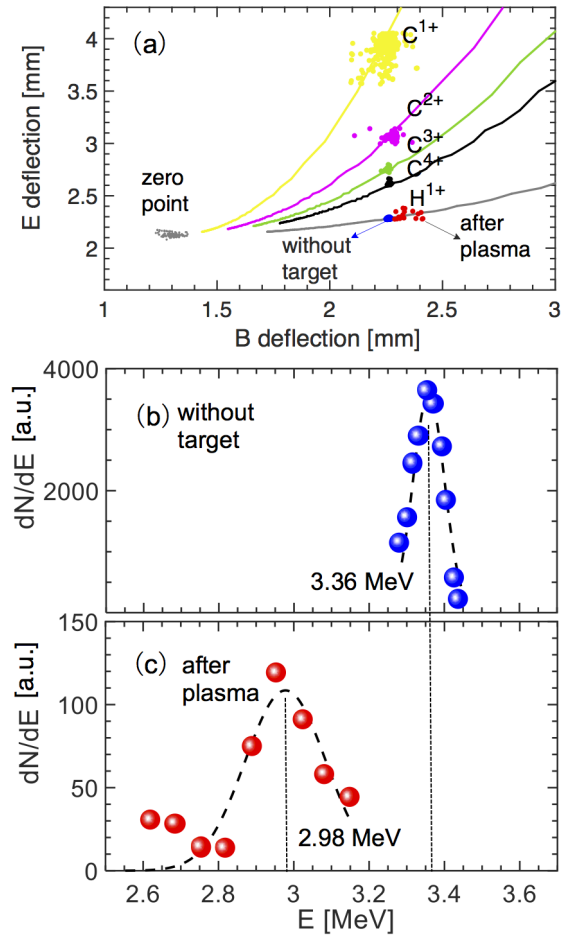


FIG. 2. **TPS CR39 tracks of quasi-monoenergetic ions passing through the system with/without target and the converted energies of protons.** (a) Tracks of ions recorded on TPS CR39 passing through null target and plasma target. The X and Y coordinates represent the magnetic and electric deflection distances. The dots with the same B deflection from up to down (yellow, magenta, green, black and blue in order) represent tracks formed by C^{1+} , C^{2+} , C^{3+} , C^{4+} and protons passing through the system without target. Tracks for protons passing through plasma are represented by red dots. The tracks for the zero reference point are indicated with grey dots. The dashed curves represent the theoretical tracks of these ion species with various energies. (b) Energy spectra of the protons passing the system without target. The experimental distribution (blue dots) are well fitted by a gaussian profile (dashed line) with central energy of 3.36 MeV (dotted line). (c) Energy spectra of the protons passing the system without target. The experimental distribution (blue dots) are fitted by a gaussian profile (dashed line) with central energy of 2.98 MeV.

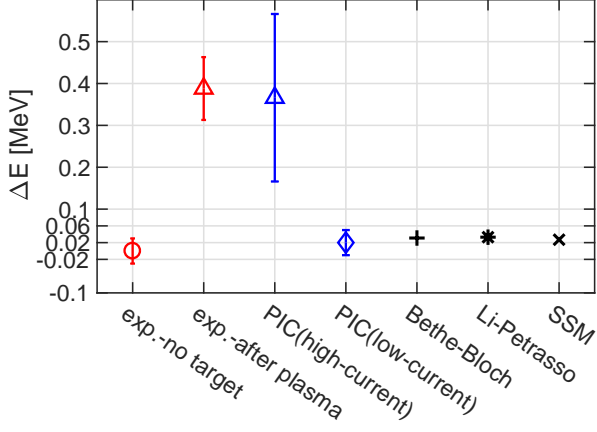


FIG. 3. **Experimental results, numerical (PIC) and analytical prediction of proton energy loss in the dense plasma target** (see text for details on plasma parameters). The experimental data (red triangle) and PIC simulation data (blue triangle for 3.2×10^7 A/cm² high-current case, blue diamond for 3.2×10^2 A/cm² low-current case) are determined as the central energy downshift, with error bars representing the FWHM of their respective energy spectra. In the analytical calculations, the incident beam energy is assumed to be monoenergetic with the same energy as the central energy of proton beam used in experiment. For comparison, the experimental data for proton beam energy without target is shown with red circle, but downshifted by its central energy.

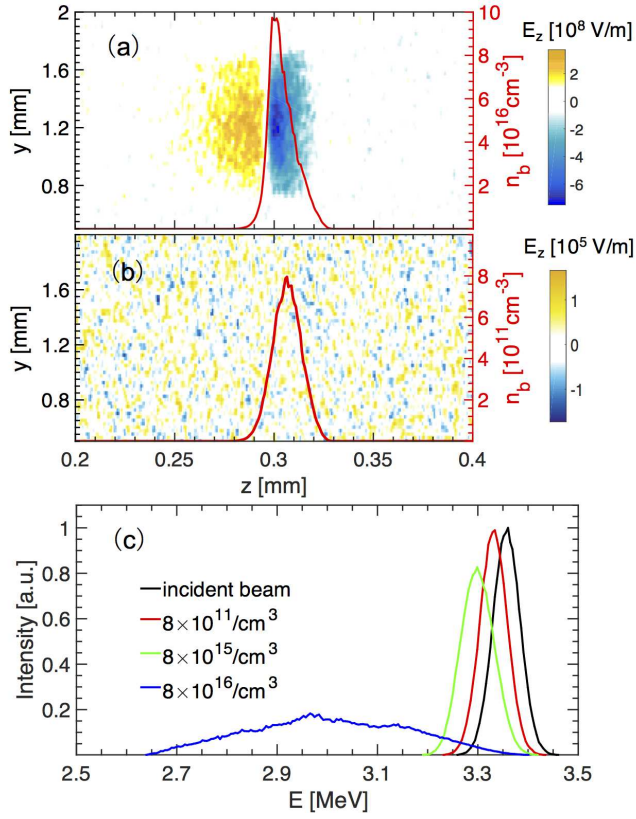


FIG. 4. Simulated distribution of longitudinal electric field and proton beam density during beam transport in experimentally used ionized target, and the resulted proton beam energy spectra shift after passing through the sample. (a) Longitudinal electric field driven by proton beam, moving along the Z direction with a beam density of 8×10^{16} cm $^{-3}$. The beam density profile is indicated by the red solid curve. (b) The same situation as in (a) but the initial beam density is reduced to 8×10^{11} cm $^{-3}$. (c) Normalized energy spectra. Incident protons without target interaction are represented by the solid black curve. The colored lines indicate the interaction with the plasma target varying the beam density from 8×10^{11} cm $^{-3}$ (red) to 8×10^{15} cm $^{-3}$ (green), and finally 8×10^{16} cm $^{-3}$ (blue).